

Stability of Biaxial Nematic Phase in Model Bent-Core Systems

Piotr Grzybowski* and Lech Longa†

Marian Smoluchowski Institute of Physics,

Department of Statistical Physics and Mark Kac Center for Complex Systems Research,

Jagellonian University, Reymonta 4, Kraków, Poland

(Dated: October 2, 2018)

Abstract

We study a class of models for bent-core molecules using low density version of Local Density Functional Theory. Arms of the molecules are modeled using two- and three Gay-Berne (GB) interacting units of uniaxial and biaxial symmetry. Dipole-dipole interactions are taken into account by placing a dipole moment along the C_2 symmetry axis of the molecule. The main aim of the study is to identify molecular factors that can help stabilizing the biaxial nematic phase. The phase diagrams involving isotropic (I), uniaxial (N_U) and biaxial (N_B) nematic phases are determined at given density and dipole strength as function of bent angle. For molecules composed of two uniaxial arms a direct $I - N_B$ phase transition is found at a single Landau point, which moves towards lower bent angles with increasing dipole magnitude. For the three-segment model strengthening of the dipole-dipole interaction results in appearance of a line of Landau points. There exists an optimal dipole strength for which this line covers the maximal range of opening angles. Interestingly, the inclusion of biaxial GB ellipsoids as building blocks reveals the direct $I - N_B$ transitions line even in a non-polar, two-arms model. The line is shifted towards higher opening angles as compared to the uniaxial case.

*e-mail address:merlin@th.if.uj.edu.pl

†e-mail address:lech.longa@uj.edu.pl

Thermotropic biaxial nematic phase, embodying the "holy grail" [1] of the liquid crystals physics, recently has engendered much scientific interest. In 2004 a long-awaited discovery was announced [2–4] and the thermotropic biaxial nematics were claimed to be found at last, 34 years after its first theoretical prediction by Freiser in 1970 [5]. The discovery was made in systems of the bent-core mesogens, also often called banana- or boomerang-shaped. They possessed a rigid bent-core with apex angle of $\sim 140^\circ$, although recently the biaxial phase has also been reported for bent-core systems with apex angle of 90° [6]. It should be noted that first experimental speculations of possible biaxiality in bent-core systems were made earlier [7].

From theoretical point of view it had been known that one can expect a biaxial phase in bent-core systems. Bifurcation analysis for hard boomerang model, with molecules composed of two hard spherocylinders joined at their ends, was carried out by Teixeira, Masters and Mulder [8] predicting phase diagrams with a direct $I - N_B$ phase transition at an isolated Landau point for apex angle of 107° . Subsequent mean-field analysis of interacting quadrupoles by Luckhurst [9] have predicted that only a bond angle within a few degrees of the tetrahedral angle (109.47°), where Landau point was observed, would allow the biaxial nematic to appear above the freezing point of a real uniaxial nematic. That raised a new question, since the experiments reported the angle to be near 140° . Among others that issue has been addressed in various simulation approaches, including Metropolis Monte Carlo study of a Lebwohl-Lasher lattice model [10]. Introduced asymmetry of molecule arms in the aforementioned paper shifted Landau point towards lower angles. The same model was used to investigate the influence of molecule flexibility [11, 12], and recently of dipole-dipole interactions [13] on phase diagram.

As it has appeared quite recently, the biaxial phase proves to be more challenging experimentally than earlier thought [14]. It seems therefore important to look into molecular models that can help in a proper understanding the biaxiality issue. In the present paper we construct a class of models of bent-core molecules with the aid of including a broad range of molecular factors that can appear relevant in stabilizing biaxial phase. We build up the molecule from parts interacting through Gay-Berne (GB) potential [15] and go beyond lattice models to account, at least partly, for excluded volume effects. We will keep the arm's length close to experimental values. The simulations for similar molecules, but with relatively short arms, have not shown any trace of the biaxial nematic phase [16–19].

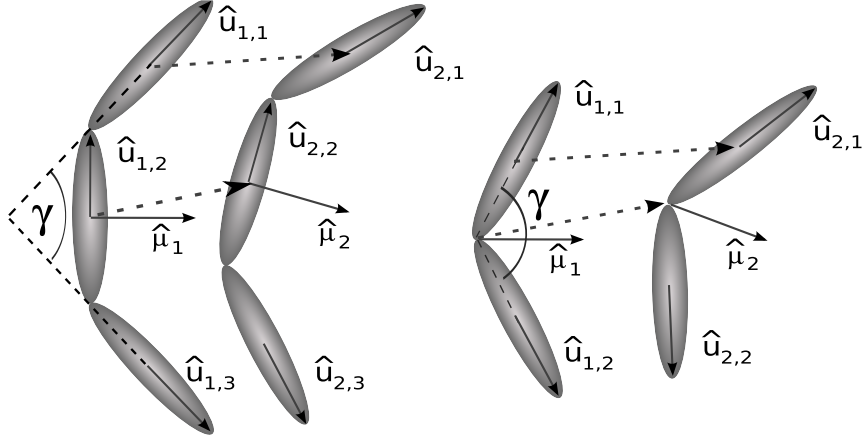


FIG. 1. The construction of pair potential out of two and three GB interacting parts firmly attached to molecule. Each part of one molecule interacts with every part from other molecule via V_{GB} . Dipole-Dipole interaction, V_{DD} , is also added.

Apart from isotropic and uniaxial nematic phase, smectic phases were observed, which is in agreement with predictions of hard spherocylinder dimer model presented in [20].

The atomistic simulations [21] of the molecular systems studied experimentally [2, 3] have confirmed the existence of a weak biaxiality in that system. Similarly, for a system of GB bent-core molecules with long arms the biaxial nematic phase was observed on cooling [22].

Our attempt in the present work is to employ the GB interaction[15, 23] to model interacting parts of the molecules. Then, the models are studied using low density approximation to the Local Density Functional theory [24, 25]. By means of bifurcation analysis [26, 27], we determine bifurcation phase diagrams for bent-cores constructed out of two and three GB parts, as shown in Fig. 1. Finally, we introduce the dipole-dipole interactions with the dipoles taken parallel to molecular C_2 symmetry axis and investigated the influence of the dipole strength on stability of N_B .

We employ reduced units by setting $\sigma_0 = 1$ and $\epsilon_0 = 1$ for the GB potential parameters [15]. The reduced distance r^* and the reduced temperature t are then given by $r^* = r/\sigma_0$ and $t = k_B T/\epsilon_0$, respectively. We also set $\nu = 1$, $\mu = 2$ [15] and choose the ratio of length to breath of 5:1 for the uniaxial arms.

The biaxial arms of bent-core molecules are modeled with the help of soft GB ellipsoids as proposed by Berardi-Fava-Zannoni [23], where for the axes we take $(\sigma_x, \sigma_y, \sigma_z) = (1.2, 0.514, 3.4)$ and for the potential parameters $(\epsilon_x, \epsilon_y, \epsilon_z) = (1.0, 1.4, 0.2)$; in addition $\mu = 1$

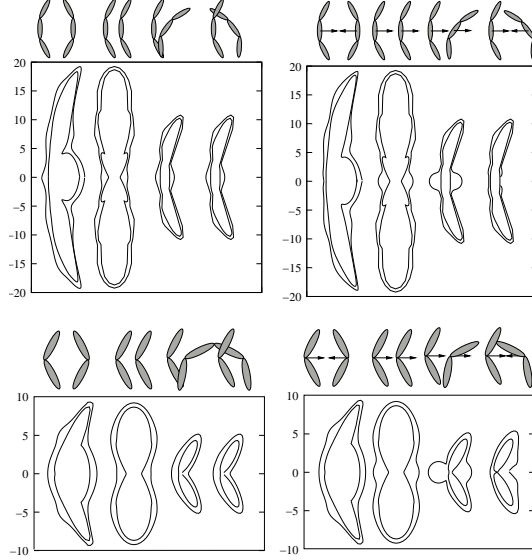


FIG. 2. Exemplary equipotential surfaces for model bent-core molecules composed of 2 (bottom) and 3 (top) uniaxial parts for arm’s elongation of 5 : 1 and for opening angle $\gamma = 126^\circ$. The case with the dipole-dipole interaction included ($\mu = 2.0$) is shown to the right. Surfaces are shown for the total pair potential equal to 0 and -0.2 .

and $\nu = 3$ (for definitions of the parameters please refer to [23]). The ellipsoids are oriented so that the shortest axis is perpendicular to the molecular symmetry plane containing molecular parts and the longest one is lying in that plane. As mentioned in [23] those parameters and orientation of the ellipsoids make the attractive forces strongest in the face-to-face configuration (that is in the direction of shorter axis). Clearly, that model exhibits molecular biaxiality in the limit of $\gamma = 180^\circ$ and $\gamma = 0.0$; there should also exist an angle separating rod-like and disk-like molecular shapes.

The resulting GB potential V_{GB} for a pair of bent-core molecules is then a sum of four terms for the two-part case and of nine terms for the three-part case. The dipole-dipole part of interaction is of standard form:

$$V_{DD}(\boldsymbol{\mu}_1, \boldsymbol{\mu}_2, \mathbf{r}) = \frac{\boldsymbol{\mu}_1 \cdot \boldsymbol{\mu}_2 - 3(\boldsymbol{\mu}_1 \cdot \mathbf{r})(\boldsymbol{\mu}_2 \cdot \mathbf{r})}{r^3},$$

where $\boldsymbol{\mu}_i = \mu \hat{\boldsymbol{\mu}}_i$, $i = 1, 2$; $\hat{\boldsymbol{\mu}}_i$ is the unit vector and μ the magnitude of $\boldsymbol{\mu}_i$. The total pair interaction, V , is the sum of V_{GB} and V_{DD} . In Fig. 2 shown are the exemplary equipotential surfaces. Figures show the profiles for four different relative molecular orientations, including two- and three GB part bent-core molecules of uniaxial arms.

TABLE I. Dipole-dipole contribution to total pair potential energy in ground state.

μ	$ V_{DD}/(V_{GB} + V_{DD}) $
2.8	0.50
2.2	0.40
1.6	0.25
1.5	0.22
1.2	0.15

Relative importance of V_{GB} and V_{DD} parts is measured by the ratio $\left| \frac{V_{DD}}{V_{GB} + V_{DD}} \right|$. The ground state values of this parameter for different values of μ are given in Table I. We study the equilibrium properties of the systems by minimizing the grand potential with respect to the one-particle distribution function p [24–27]. The necessary condition is given by a self-consistent integral equation for stationary distribution $p_S(q)$. It reads [27]

$$p_S(q) = Z_S^{-1} \exp\{C_1(q, [p_S])\}, \quad (1)$$

where $Z_S = \int \exp\{C_1(q, [p_S])\} dq / \langle N \rangle$ is the normalization constant, $C_1(q, [p_S])$ is the one-particle direct correlation function, $\langle N \rangle$ is the average number of particles in the system and q represents collectively all degrees of freedom of a single molecule.

In the present study we (a) approximate C_1 using second order virial expansion, sometimes also referred to as low density approximation and (b) restrict analysis to nematics, which amounts in setting $p_S(q) = \rho P(\mathbf{\Omega})$, where $\rho = \frac{\langle N \rangle}{V} \sigma_0^3$ is the dimensionless density and $\mathbf{\Omega}$ are the Euler angles parameterizing orientation of a molecule-fixed frame with respect to the laboratory-fixed frame. After these limitations the Eq. (1) becomes:

$$P(\mathbf{\Omega}_1) = Z^{-1} \exp \left[\rho \int c_2(\mathbf{\Omega}_1 \mathbf{\Omega}_2) P(\mathbf{\Omega}_2) d\mathbf{\Omega}_2 \right], \quad (2)$$

with

$$c_2(\mathbf{\Omega}_1 \mathbf{\Omega}_2) \equiv \int \left\{ \exp \left[-\frac{1}{t} V(\mathbf{\Omega}_1^{-1} \mathbf{\Omega}_2, \mathbf{r}_{12}^*) \right] - 1 \right\} d^3 \mathbf{r}_{12}^*,$$

and normalization constant:

$$Z = \int \exp \left[\rho \int c_2(\mathbf{\Omega}_1 \mathbf{\Omega}_2) P(\mathbf{\Omega}_1) d\mathbf{\Omega}_1 \right] d\mathbf{\Omega}_2.$$

Here $d\Omega = d\alpha d(\cos(\beta)) d\gamma$ stands for integration over Euler angles, $d^3\mathbf{r}^* = r^{*2}dr^* d(\cos(\theta)) d\phi$ and $\Omega_1^{-1}\Omega_2$ is the relative orientation of the molecules.

The usual expansions of $P(\Omega)$ in the base of D_{2h} symmetry adapted Δ functions [26]

$$P(\Omega) = \sum_{L,m,n} \frac{2L+1}{8\pi^2} \overline{\Delta_{m,n}^{(L)}} \Delta_{m,n}^{(L)}(\Omega) \quad (3)$$

allows to introduce the order parameters $\overline{\Delta_{m,n}^{(L)}} = \int d\Omega P(\Omega) \Delta_{m,n}^{(L)}(\Omega)$ for nematics. The summation runs over the allowed values of $\{L, m, n\}$, where L is a non-negative integer. Generally, if L is even, then $0 \leq m \leq L$ and $0 \leq n \leq L$. If L is odd, then $2 \leq m \leq L$ and $2 \leq n \leq L$. If, in addition, we expand c_2 :

$$c_2(\Omega_1\Omega_2) = \sum_{L,m,n} c_{mn} \Delta_{m,n}^{(L)}(\Omega_1^{-1}\Omega_2)$$

where

$$c_{mn} = \frac{2L+1}{8\pi^2} \int d\Omega_1^{-1}\Omega_2 c_2(\Omega_1\Omega_2) \Delta_{m,n}^{(L)}(\Omega_1^{-1}\Omega_2)$$

and where $c_{mn} = c_{nm}$ due to particle interchange symmetry, then Eq. (2) becomes reduced to the set (in general infinite) of nonlinear equations for the order parameters. Using bifurcation analysis we now seek for a subset of nonzero order parameters, describing low-symmetry phase, that branch off from the background high-symmetry phase. Generally, in the isotropic phase all order parameters vanish. The uniaxial phase is characterized by nonzero order parameters indexed by $m = 0$. Finally, in the biaxial nematic phase all the order parameters become nonzero.

The bifurcation points so determined are either spinodal points for the first-order phase transitions or critical points for the continuous transitions. Hence, for continuous and weakly first-order phase transitions, as holds of isotropic and nematic phases, we arrive at quite accurate estimates of the phase diagrams in temperature-density plane. Following the analysis as described in [27] two different bifurcation formulas can be derived. The first one is the equation for the bifurcation from the isotropic phase. It reads

$$\rho = \frac{10}{c_{00} + c_{22} - \sqrt{4c_{02}^2 (c_{00} - c_{22})^2}}. \quad (4)$$

For the uniaxial to biaxial bifurcation a more complex formula is found

$$\rho = 35 \left[\frac{2c_{00}(adc_{02} - d) + c_{02}(2a + abc_{22}) - d^2c_{00} + bc_{22}}{(a^2 + 2bd)(c_{02}^2 + c_{00}c_{22})} - \frac{\sqrt{a^2c_{00}c_{22} + bd(c_{00}c_{22} - 2c_{02}^2)}}{(a^2 + 2bd)(c_{02}^2 + c_{00}c_{22})} \right], \quad (5)$$

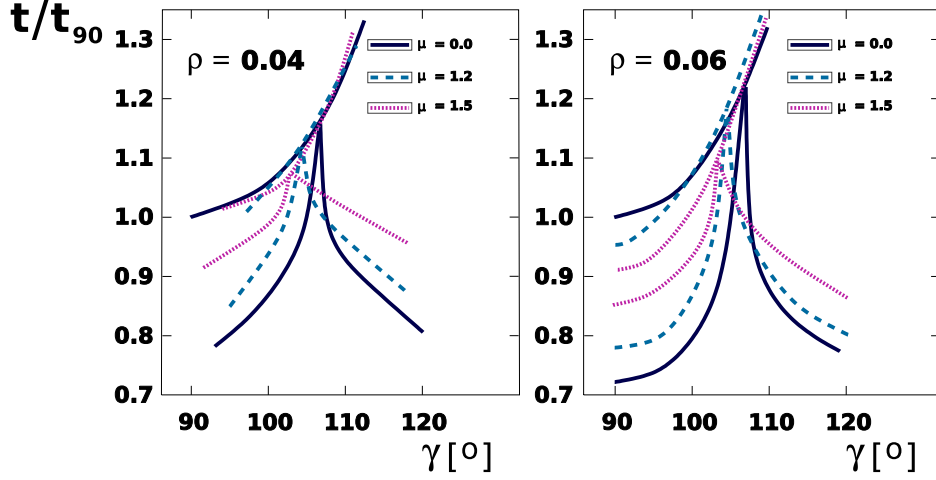


FIG. 3. Diagrams for two-parts banana, for two densities (ρ) and three values of dipole moment (μ). On each plot two branches of bifurcation from uniaxial to biaxial phase meet the upper line of bifurcations from isotropic phase.

where

$$\begin{aligned}
 a &= 20\overline{\Delta_{0,2}^{(2)}} + \sqrt{15}\overline{\Delta_{0,2}^{(4)}}, \\
 b &= 14 + 20\overline{\Delta_{0,0}^{(2)}} + \overline{\Delta_{0,0}^{(4)}} + \sqrt{35}\overline{\Delta_{0,4}^{(4)}}, \\
 d &= 7 - 10\overline{\Delta_{0,0}^{(2)}} + 3\overline{\Delta_{0,0}^{(4)}},
 \end{aligned}$$

and where $\overline{\Delta_{m,n}^{(L)}}$ are determined in the uniaxial nematic phase. We would like to point out that since the formulas for $\overline{\Delta_{m,n}^{(L)}}$ s depend on ρ , the equation (5) for given t becomes a self-consistent equation for density.

Please note that each c_{mn} is a six dimensional integral. We performed numerical integration to obtain temperature dependence for each of the coefficients for given set of the molecular parameters. The integration procedure was implemented in C. We have incorporated both Monte Carlo and adaptive multi-point Gauss quadratures method in the integration procedure. We performed Monte Carlo (MC) integration over orientations using quaternion parametrization of rotations and then calculated the integral over length of intermolecular vector \mathbf{r}_{12} using adaptive Gauss quadratures. Approximately 2 million of MC cycles were used to calculate the integral; the relative error was estimated to be less than 1%. Now we present the bifurcation diagrams, which follow from the solutions of the bifurcation equations (4) and (5) for the uniaxial V_{GB} . In Fig. 3 and 4 we have plotted t divided by t_{90} , the temperature of bifurcation from isotropic phase for $\gamma = 90^\circ$ in the

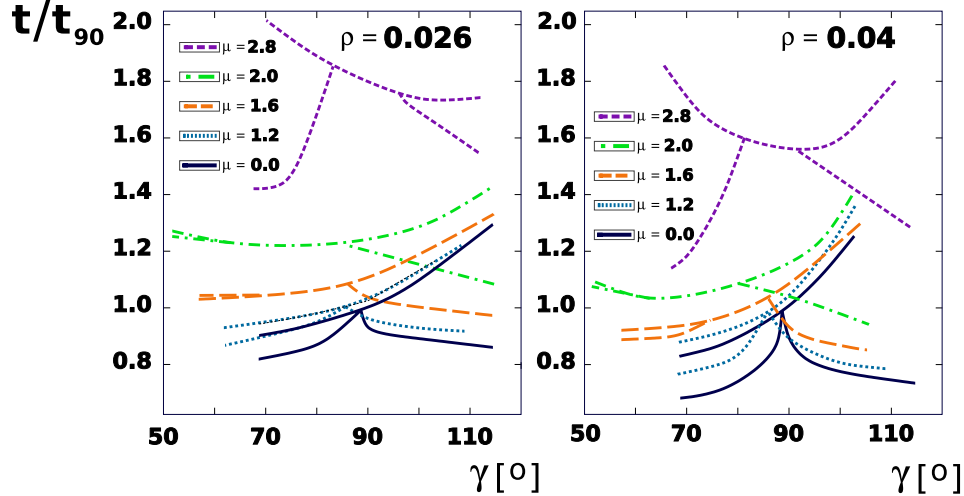


FIG. 4. Diagrams for three-parts banana, for two densities, and five dipole moments. Each plot shows the bifurcation from isotropic phase and two lower branches of uniaxial-to-biaxial phase transition.

TABLE II. Bifurcation temperatures from isotropic phase for $\gamma = 90^\circ$.

ρ	t_{90}
bent-core molecule composed of two parts:	
0.04	0.84
0.06	0.96
bent-core molecule composed of three parts:	
0.026	1.34
0.04	1.71

non-polar case. Numerical values of t_{90} are gathered in Table II. Note that the standard phase sequence [8] is recovered that involves the isotropic phase, the rod-like and disc-like uniaxial nematic phase and the biaxial nematic phase. For the case of two-part molecule without the dipole moment Landau point is found to be near $\gamma = 107^\circ$, in agreement with the hard-boomerang model [8]. The diagrams include two dipole strengths $\mu = 1.2$ and $\mu = 1.5$ for which dipole-dipole interaction is about 15% and 22%, respectively, of the total potential in ground state. The bicritical point is shifted towards lower angles with increasing μ , which contrasts with the results of Monte Carlo simulation for the Lebwohl-Lasher lattice model[13], where introduction of the dipoles resulted in a line of direct isotropic-biaxial

TABLE III. Landau point versus dipole magnitude μ

μ	Landau point
bent-core molecule composed of two parts:	
0.0	107°
1.2	104°
1.5	103°
bent-core molecule composed of three parts:	
	$\rho=0.026$ $\rho=0.04$
0.0	89° 89°
1.2	86° 86°
1.6	74° - 86° 74° - 86°
2.0	63° - 86° 63° - 80°
2.8	83° - 97° 82° - 92°
bent-core molecule composed of two biaxial ellipsoids :	
0.0	121° - 128°

transitions.

For the non-polar three-part molecule, the Landau point is found to be at $\gamma = 89^\circ$ and is shifting to lower angles with increasing dipole magnitude (Table III) up to a point where the dipole-dipole interactions make up 20% ($\mu = 1.4$) of the total potential in the ground state. Above that value the bicritical point changes into a line of Landau points that widens with increasing μ ; for $\mu = 1.6$ it covers the range of 12° and for $\mu = 2.0$ it extends for more than 20° .

The low γ boundary practically does not change (for lower density) and is equal to 86° for the dipole strength $\mu \leq 2.1$. Then the bicritical region begins to shrink and is shifted towards higher angles. The highest dipole studied was the one of $\mu = 2.8$ for which V_{DD} approaches 50% of the total potential energy. As can be seen from Fig. 3 the bicritical line in that case is still getting shorter and moves towards higher bond angles. Fig. 6 shows the evolution of Landau region as function of the dipole magnitude, μ .

The diagrams are presented for two densities such that the corresponding packing fraction is of the order of 0.3–0.4. As can be seen from Table III some differences appear with varying

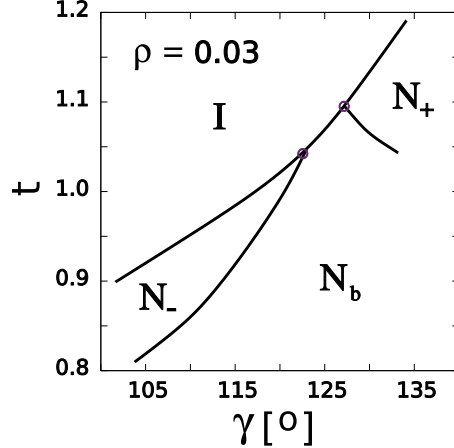


FIG. 5. Bifurcation diagram for non-polar bent-core molecules modeled by two biaxial GB ellipsoids [23].

density for the strongest dipoles ($\mu \geq 2.0$). Namely the line of the direct isotropic-biaxial transitions shrinks for higher density.

Finally we take into account the model where the arms of the molecules are biaxial. We are going to address the issue of observed disagreement between the angles for which the Landau point appears experimentally ($\gamma = 140^\circ$) and theoretically. Results presented below replace uniaxial GB arms with their biaxial version developed by Fava, Berardi and Zannoni [23]. Interestingly, the Landau point in the biaxial model, Fig. 5, is replaced by a line of bicritical points even for the non-polar molecule. That line starts near 121° and ends for $\gamma = 128^\circ$. The region becomes reduced to a single point with decreasing arm's biaxiality.

Summarizing, we have presented a bifurcation study for a class of models with characteristic features typical of the bent-core molecule. Using Density Functional Theory we have retrieved the diagrams in low density approximation. Analysis included two and three-part bend-cores with arms modeled by GB interacting ellipsoids of uniaxial and biaxial symmetry. The dipole-dipole interaction was added and the dipole strength influence studied. Non-polar uniaxial model revealed a single Landau point, in agreement with results for hard molecules [8]. The deviation from uniaxial symmetry of the arms resulted in transformation of the single bicritical point into a line of direct isotropic-biaxial transitions. The inclusion of the dipole-dipole interactions resulted in shifting of the Landau point towards lower bond angles with increasing dipole magnitude. For the case of two-arm molecule stronger dipoles easier destabilized uniaxial nematic phase. For the three-part banana a line of the bicriti-

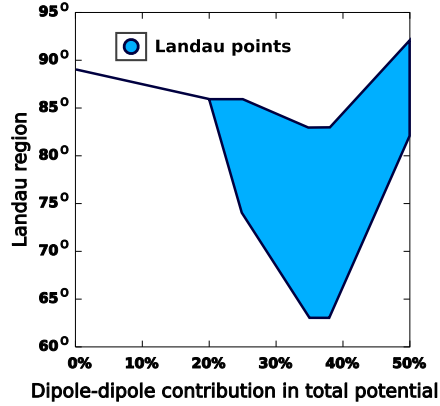


FIG. 6. The range of direct isotropic-biaxial transitions in bend angle, in function of dipole-dipole contribution in total potential.

cal points has emerged. The results suggest that there exists an optimal dipole range that makes the appearance of the biaxial phase most probable.

ACKNOWLEDGMENTS

Authors wish to thank Paweł F. Góra and Michał Cieśla for useful discussions. The work was supported by grant from MNiSW no N202 169 31/3455. The numerical analysis was performed using computer cluster at ICM under grant G27-8.

-
- [1] G. R. Luckhurst, *Nature* **430**, 413 (2004).
 - [2] L. A. Madsen, T. J. Dingemas, M. Nakata, and E. T. Samulski, *Phys. Rev. Lett.* **92**, 145505 (2004).
 - [3] B. R. Acharya, A. Primak, and S. Kumar, *Phys. Rev. Lett.* **92**, 145506 (2004).
 - [4] K. Severing and K. Saalwachter, *Phys. Rev. Lett.* **92**, 125501 (2004).
 - [5] M. J. Freiser, *Phys. Rev. Lett.* **24**, 1041 (1970).
 - [6] M. Lehmann, S.-W. Kang, C. Kohn, S. Haseloh, U. Kolb, D. Schollmeyer, Q. Wang, and S. Kumar, *J. Mater. Chem.* **16**, 4326 (2006).
 - [7] T. J. Dingemans and E. T. Samulski, *Liq. Cryst.* **27**, 131 (2000).
 - [8] P. I. C. Teixeira, A. J. Masters, and B. M. Mulder, *Mol. Cryst. Liq. Cryst.* **323**, 167 (1998).
 - [9] G. R. Luckhurst, *Thin Solid Films* **393**, 40 (2001).

- [10] M. A. Bates and G. R. Luckhurst, Phys. Rev. E **72**, 051702 (2005).
- [11] M. A. Bates, Phys. Rev. E **74**, 061702 (2006).
- [12] L. Longa, G. Pająk, and T. Wydro, Phys. Rev. E **76**, 011703 (2007).
- [13] M. A. Bates, Chem. Phys. Lett **437**, 189 (2007).
- [14] K. V. Le, M. Mathews, M. Chambers, J. Harden, Q. Li, H. Takezoe, and A. Jkli, Phys. Rev. E **79**, 030701R (2009).
- [15] J. G. Gay and B. J. Berne, J. Chem. Phys. **74** (1981).
- [16] S. J. Johnston, R. J. Low, and M. P. Neal, Phys. Rev. E **66**, 061702 (2002).
- [17] S. J. Johnston, R. J. Low, and M. P. Neal, Phys. Rev. E **65**, 051706 (2002).
- [18] R. Memmer, Liq. Cryst. **29**, 483 (2002).
- [19] S. Orlandi, R. Berardi, J. Stelzer, and C. Zannoni, J. Chem. Phys. **124**, 124907 (2006).
- [20] Y. Lansac, P. K. Maiti, N. A. Clark, and M. A. Glaser, Phys. Rev. E **67**, 011703 (2003).
- [21] J. Pelaez and M. R. Wilson, Phys. Rev. Lett. **97**, 267801 (2006).
- [22] W. Józefowicz and L. Longa, arXiv: **0904.0666v1** (2009).
- [23] R. Berardi, C. Fava, and C. Zannoni, Chem. Phys. Lett **236**, 462 (1995).
- [24] R. Evans, Adv. Phys. **28**, 143 (1979).
- [25] J. P. Hansen, *Observation, Prediction and Simulation of Phase Transitions in Complex Fluids* (Kluwer, Dordrecht, 1995).
- [26] B. Mulder, Phys. Rev. A **39**, 360 (1989).
- [27] L. Longa, P. Grzybowski, S. Romano, and E. Virga, Phys. Rev. E **71**, 051714 (2005).